

See discussions, stats, and author profiles for this publication at: <https://www.researchgate.net/publication/51677625>

Formation of Self-Assembled Chains of Tetrathiafulvalene on a Cu(100) Surface

ARTICLE in THE JOURNAL OF PHYSICAL CHEMISTRY A · SEPTEMBER 2011

Impact Factor: 2.69 · DOI: 10.1021/jp205085s · Source: PubMed

CITATIONS

3

READS

24

9 AUTHORS, INCLUDING:



[J. Rodríguez-Fernández](#)

Aarhus University

14 PUBLICATIONS 75 CITATIONS

[SEE PROFILE](#)



[José M Gallego](#)

Spanish National Research Council

84 PUBLICATIONS 1,876 CITATIONS

[SEE PROFILE](#)



[Roberto Otero](#)

Universidad Autónoma de Madrid

60 PUBLICATIONS 2,004 CITATIONS

[SEE PROFILE](#)



[Manuel Alcami](#)

Universidad Autónoma de Madrid

146 PUBLICATIONS 2,048 CITATIONS

[SEE PROFILE](#)

Formation of Self-Assembled Chains of Tetrathiafulvalene on a Cu(100) Surface

Yang Wang,^{*,†} Christian Urban,[‡] Jonathan Rodríguez-Fernández,[‡] José M. Gallego,^{§,||} Roberto Otero,^{‡,||} Nazario Martín,^{⊥,||} Rodolfo Miranda,^{‡,||} Manuel Alcami,[†] and Fernando Martín^{†,||}

[†]Departamento de Química C-13, Universidad Autónoma de Madrid, Cantoblanco, Madrid, Spain

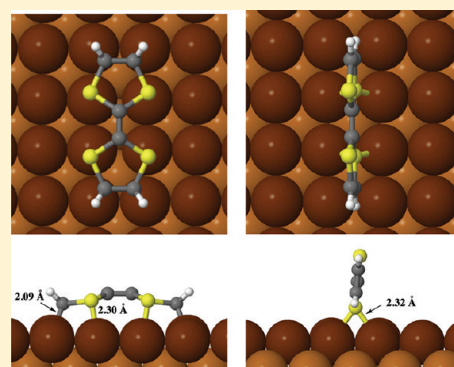
[‡]Departamento de Física de la Materia Condensada, Universidad Autónoma de Madrid, Cantoblanco, Madrid, Spain

[§]Instituto de Ciencia de Materiales de Madrid - CSIC, Cantoblanco, Madrid, Spain

^{||}Instituto Madrileño de Estudios Avanzados en Nanociencia (IMDEA-Nanociencia), Cantoblanco, Madrid, Spain

[⊥]Departamento de Química Orgánica, Facultad de Química, Universidad Complutense de Madrid, Madrid, Spain

ABSTRACT: Formation of self-assembled chains of tetrathiafulvalene (TTF) on the Cu(100) surface has been investigated by scanning tunneling microscopy and density functional theory calculations that include semiempirical van der Waals (vdW) interaction corrections. The calculations show that the chain structures observed in the experiments can only be explained by including the vdW interactions. The molecules are tilted along the chain in order to achieve maximal intermolecular interaction. The chains are metastable on the surface, which is consistent with the experimental observation that they disappear after annealing. The fact that all TTF chains observed in the experiment are short might be possibly explained by the interplay between the stabilizing vdW molecule–molecule interaction and the destabilizing rearrangement of surface atoms due to the strong molecule–substrate interaction.



INTRODUCTION

A large variety of studies have been dedicated to the search of new materials in order to improve the efficiency of organic photovoltaic solar cells (OPVCs).^{1,2} In these solar cells, organic molecules, typically electron donors and acceptors, are mixed up to form a polymer blend.^{3,4} The adsorption and self-assembly of these organic molecules play an important role in determining electronic properties and morphology of the adsorbates, which is crucial to improve the solar cell efficiency. In experiments, organic molecules are deposited in ultrahigh vacuum (UHV) conditions onto metal surfaces and, when the coverage is high enough, they may form a self-assembled overlayer.^{5,6} This overlayer can be further observed and even manipulated by using scanning tunneling microscopy (STM), thus providing us with valuable information on the overlayer structures formed by the molecules.⁷

Among the molecule candidates for OPVCs, tetrathiafulvalene (TTF) is one of the most commonly used electron donors. TTF and tetracyano-*p*-quinodimethane (TCNQ, an electron acceptor) can form a charge-transfer salt. This well-known conducting organic crystal has spawned a new field of organic electronics.⁸ Recent STM experiments observed that TTF on Au(111) surface forms molecular arrays spaced by a few nanometers, due to the long-range repulsive potential.⁹ Density functional theory (DFT) calculations demonstrated the electrostatic nature of the long-range interactions, induced by the charge accumulation in the molecules upon chemisorption.⁹ Adsorption of a single TTF

molecule has also been investigated by means of DFT calculations for other metal surfaces, including the unreconstructed (111) surfaces of gold, silver, and copper,¹⁰ as well as the (110) surfaces of gold¹¹ and silver,^{11,12} for which there are no experimental measurements to compare with. In addition to this, very recently, the adsorption of a TTF derivative, 2-[9-(1,3-dithiol-2-ylidene)anthracen-10(9H)-ylidene]-1,3-dithiole (exTTF), on Au(111) has been investigated both experimentally and theoretically.¹³ As for pure TTF molecules, the calculations for exTTF made use of standard DFT methods. Despite the above-mentioned theoretical efforts, none of the reported DFT calculations describing adsorption of TTF or its derivatives has included the effect of van der Waals (vdW) forces. However, these forces have been revealed to play an important role in the observed geometries and adsorption energies of aromatic molecules adsorbed on metal surfaces.¹⁴

The present work aims at studying the formation of self-assembled chains of TTF on Cu(100) both experimentally and theoretically. In the experiments, TTF deposited on Cu(100) at room temperature in a UHV environment exhibits, at low coverage (0.2 ML), well-ordered chain-like structures of molecules.

Special Issue: Richard F. W. Bader Festschrift

Received: May 31, 2011

Revised: September 16, 2011

Published: September 28, 2011

To understand these observations we have computationally investigated the TTF/Cu(100) system by performing DFT calculations that include vdW corrections.

The paper is organized as follows. In the following two sections, experimental and computational methods are briefly described. Then the results are presented and discussed on the light of the DFT + vdW calculations. In particular, the formation of self-assembled TTF on Cu(100) is discussed in detail. Conclusions are drawn in the final section of the paper.

METHODS

Experimental Approach. The growth of TTF on Cu(100) and the STM measurements were carried out in a UHV chamber, with a base pressure of $<2 \times 10^{-10}$ Torr, equipped with standard facilities for metal surface preparation, a low-temperature effusion cell and an Aarhus-type variable-temperature (down to 80 K) fast scanning STM purchased from SPECS. Atomically flat, crystalline Cu(100) surfaces were prepared by standard sputter/anneal procedures (sputter with 1 kV Ar⁺ ions for 15 min followed by annealing to 800 K for another 15 min), which resulted in large terraces (about 200 nm wide), separated by monatomic steps. The molecules were deposited from a low-temperature Knudsen cell, working at about 10 K above room temperature, onto the clean Cu(100) substrate, that was held at room temperature. STM measurements were carried out at low temperature (~ 150 K). Tunnelling conditions were chosen so as not to disturb individual molecules ($I \approx 100$ –500 pA).

Computational Details. The calculations are performed in the framework of DFT using the Vienna ab initio simulation package (VASP).^{15–17} The projector-augmented wave (PAW) method^{18,19} is applied for describing the effective potential of core electrons. The generalized gradient approximation (GGA) is employed with the exchange–correlation functional of Perdew, Burke, and Ernzerhof (PBE).²⁰ To solve the Kohn–Sham equations, plane waves with a cutoff energy of 450 eV are used for the expansion of eigenfunctions. The occupation of electronic states is calculated using a Methfessel–Paxton smearing²¹ of 0.2 eV. For the single molecule adsorption models, the Brillouin-zone integrations are carried out using a Monkhorst–Pack grid²² for k -points sampling. The atomic positions of ions are optimized using a conjugated-gradient algorithm until the forces on each ion are smaller than $0.02 \text{ eV } \text{\AA}^{-1}$.

Considering that the standard DFT method is not capable of properly describing vdW interactions between molecule and substrate¹⁴ or between molecules,²³ a dispersion correction term (E_{disp}) is added to the DFT energy (E_{DFT}). Namely, the corrected total energy can be expressed as

$$E_{\text{tot}} = E_{\text{DFT}} + E_{\text{disp}} \quad (1)$$

During each self-consistent iteration of geometry optimization, the dispersion correction is taken into account to evaluate both the total energy and the forces on each ion.

In our VASP calculations, the dispersion corrections follow Grimme's DFT-D scheme.²⁴ Since the vdW interaction is basically a long-range dynamical dipole–dipole interaction, the dispersion correction term, E_{disp} , can be evaluated utilizing semiempirical pair potentials, i.e.,

$$E_{\text{disp}} = -s_6 \sum_{i=1}^{N-1} \sum_{j=i+1}^N \frac{C_6^{ij}}{R_{ij}^6} f_{\text{damp}}(R_{ij}) \quad (2)$$

where s_6 is a scaling factor depending on the functional in question, N is the total number of atoms, R_{ij} is the distance between atoms i and j , and the parameter C_6^{ij} describes the strength of the dispersion interaction between atoms i and j . The parameter C_6^{ij} can be evaluated as $(C_6^i C_6^j)^{1/2}$, where C_6^i is a semiempirical parameter optimized for each type of element. The damping function $f_{\text{damp}}(R_{ij})$ eliminates the dispersion correction at short distance where the DFT energy works well for short-range interaction. All the parameters in our calculations are taken as the recommended values in ref 24, as implemented in the VASP code.

The clean Cu(100) surface is modeled by a four-layer slab placed in a 3D periodic cell, separated by 13 interlayer distances (24.5 Å) of vacuum in the surface normal direction. The slab of the (100) surface is cut from the bulk structure of face-centered cubic copper crystal whose lattice parameter is optimized to be 3.64 Å, in good agreement with the experimental value of 3.614 Å.²⁵ Then, the geometry of the slab is optimized by relaxing the uppermost two layers while fixing the lowermost two layers. The geometry optimization for a single TTF molecule in the gas phase is performed by placing the molecule in a $25 \text{ \AA} \times 25 \text{ \AA} \times 25 \text{ \AA}$ periodic box, using a $3 \times 3 \times 3$ k -point mesh.

To simulate the adsorbed phases of TTF on Cu(100) surface, the molecule with the optimized geometry in gas phase is initially placed onto the four-layer slab with the same structure as in the optimized clean (100) surface. During the geometry optimization of the combined TTF/Cu(100) systems, all degrees of freedom of the adsorbed molecule and the uppermost two layers of the slab are allowed to relax. Two different sizes of supercell are used for the TTF/Cu(100) systems. A 5×5 unit cell with a $3 \times 3 \times 1$ k -point sampling is used for a single molecule adsorbed on the surface, while a 2×5 cell using a $7 \times 3 \times 1$ k -point mesh is considered to model the self-assembled chain of molecules on the surface. In the latter model, the distance between two neighboring molecules is about 5.1 Å, in agreement with the estimated experimental value, 5.0 ± 0.3 Å.

The adsorption energy of the adsorbate on the surface is defined as

$$E_{\text{ad}} = (E_{\text{mol}} + E_{\text{surf}}) - E_{\text{tot}} \quad (3)$$

where E_{tot} , E_{mol} , and E_{surf} are the total energy of the combined system of the molecule adsorbed on the surface, the energy of the isolated molecule in gas phase, and the energy of the clean surface, respectively. According to this definition, a positive value of E_{ad} corresponds to an exothermic adsorption process.

In order to estimate atomic charges and verify the bonding nature between two atoms, topological analyses of the electron density (including the core charge) are carried out based on Bader's atoms-in-molecules (AIM) theory^{26–28} by using the Bader analysis program²⁹ for VASP.

EXPERIMENTAL OBSERVATIONS

Following submonolayer deposition of TTF molecules on Cu(100) two different features can be observed by STM at room temperature, isolated dim protrusions surrounded by a dark halo, and well-organized one-dimensional (1D) chains of brighter protrusions oriented along the high-symmetry directions of the Cu(100) surface. The lack of aggregation of the dim protrusions can be attributed to the absence of molecular diffusion, which points toward a rather strong molecule–substrate interaction. On the contrary, the aggregation of the brighter species into 1D

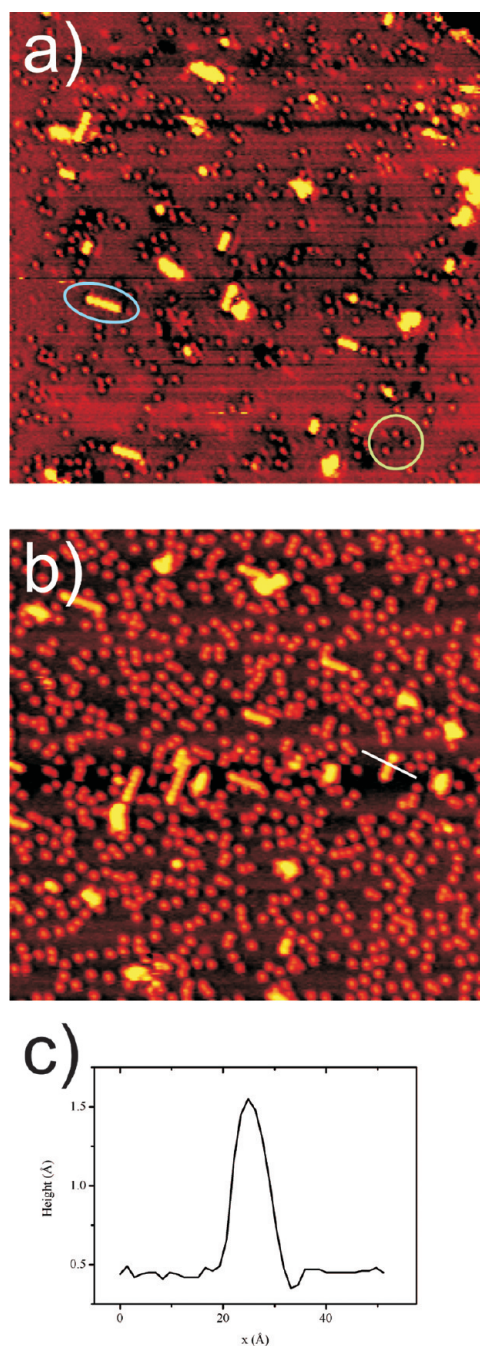


Figure 1. (a) STM image of 0.3 ML TTF on Cu(100) ($60 \times 60 \text{ nm}^2$, $V_{\text{bias}} = -2.1 \text{ V}$, $I_t = 0.8 \text{ nA}$) showing two different kind of features: 1D chains of bright molecules (blue oval) and isolated dimer protrusions surrounded by a dark halo (green circle). Basically the same behavior is observed for higher coverages in panel b ($60 \times 60 \text{ nm}^2$, $V_{\text{bias}} = -2.0 \text{ V}$, $I_t = 0.3 \text{ nA}$). Panel c shows a scan line across the 1D chains.

rods speaks of a rather high molecular mobility, and thus, a more moderate molecule substrate interaction.

Increasing the molecular coverage leads to larger numbers of both dim and bright molecular species, but no significant change in the ratio between the two species can be observed. For high coverages even the dim molecular units start to organize into a random tiling with short-range square ordering. Intermolecular distances between the dim molecular units in the ordered regions

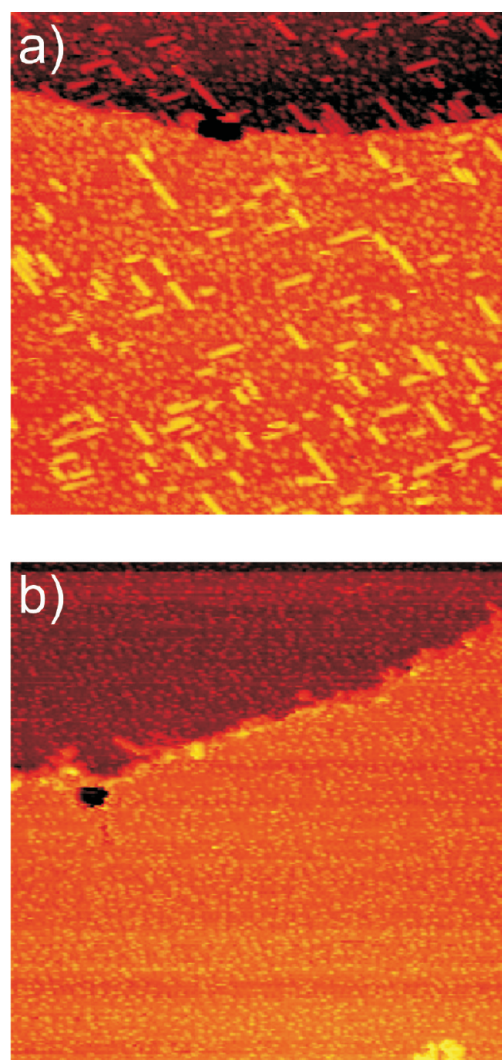


Figure 2. While the ratio between bright and dim molecules remains constant with increasing coverage, it depends on the substrate temperature. (a) STM image ($35 \times 35 \text{ nm}^2$, $V_{\text{bias}} = -1.2 \text{ V}$, $I_t = 0.3 \text{ nA}$) of a sample of about 0.4 ML TTF after room temperature deposition. 1D chains can be observed immediately after the deposition but disappear after annealing to 150°C as shown in panel b ($35 \times 35 \text{ nm}^2$, $V_{\text{bias}} = -0.8 \text{ V}$, $I_t = 0.2 \text{ nA}$).

are about 5.3 Å , i.e., about two copper unit cell vectors. Such area is, however, too small to host an intact TTF molecule. We thus speculate that the dim molecular species are fragments of dissociated TTF molecules. For the bright species there are, however, no such space limitations. Along the chains the protrusions are separated again by two atomic distances of Cu(100), but they are not observed to aggregate laterally. The average width, measured as the full width at half-maximum (fwhm) of the scan line in Figure 1, is about 8 Å . As will be discussed below in the theory section, we attribute such chains to π -stacked, standing-up, intact TTF molecules.

The ratio between reacted and standing up molecules can be tuned by changing the substrate's temperature during deposition with postdeposition annealing treatments. While deposition of TTF molecules at room temperature leads to the coexistence of both molecular species as shown in Figure 1 and Figure 2a, annealing to 150°C makes all the bright molecules disappear

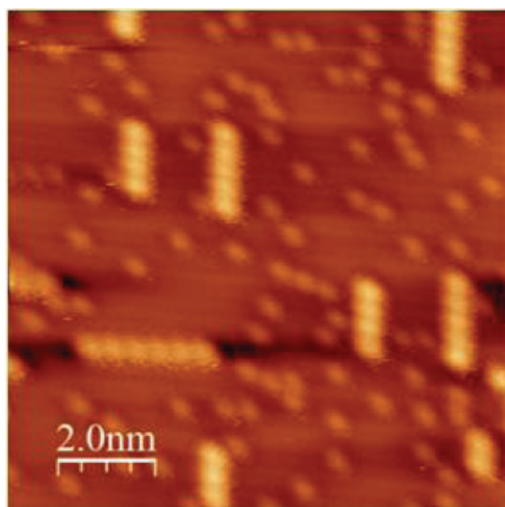


Figure 3. STM image for TTF/Cu(100) at room temperature.

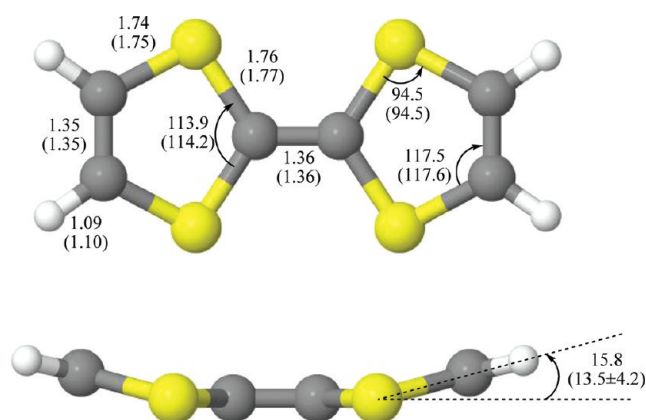


Figure 4. Optimized geometry for a single TTF molecule in gas phase. Bond lengths and bond angles are in angstroms and degree, respectively. Numbers without and with parentheses are from our DFT calculations and from gas-phase electron diffraction measurements,³² respectively. Black: carbon; yellow: sulfur; white: hydrogen.

from the surface, together with the 1D chains (see Figure 2b). This fact prevents the use of annealing procedures to lengthen the chains by Ostwald ripening processes. The longest chain that was ever observed in our STM investigations is eight molecules long.

In summary, as shown by our STM images, TTF deposited on Cu(100) at room temperature in a UHV environment exhibits well-ordered chain-like structures of molecules. An example is given in Figure 3, where the chains correspond to the brightest spots. All chains are short, the longest ones consisting of only eight molecules, and are aligned along the high symmetry directions ([100] and [010]) of the surface. Further annealing at higher temperatures leads to disappearance of the chains.

THEORETICAL RESULTS AND DISCUSSION

Single TTF Molecule in Gas Phase. For a single TTF molecule in gas phase, the optimized geometry at the equilibrium ground state is shown in Figure 4. Our DFT results are in good agreement with previous theoretical results,^{11,30,31} and with gas-phase electron diffraction measurements (see Figure 4).³²

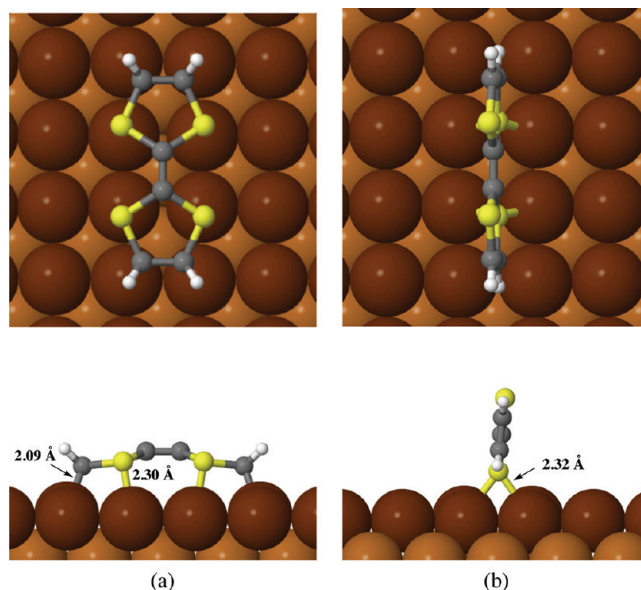


Figure 5. DFT-D optimized geometry of a single TTF on Cu(100) surface for (a) the “lying-down” and (b) the “standing-up” adsorption modes. The upper and lower panels show top and side views, respectively. The optimized bond lengths in the equilibrium geometry are also indicated.

The structure of an isolated TTF molecule in gas phase is not planar. Instead, it adopts a boat-like shape with a C_{2v} point group symmetry where the two pentagonal rings are slightly bent with a bending angle of about 15° , as illustrated in Figure 4. The preference of the neutral molecule for the nonplanar conformation can be understood by the π -electron structure of the molecule. In the planar configuration of the molecule, a π -conjugated system is formed by connecting the p-orbitals perpendicular to the molecular plane. Since each carbon atom and each sulfur atom provide one and two p-electrons, respectively, there are 14 π -electrons delocalized in the conjugated system. Therefore, each five-membered ring contains seven π -electrons, indicating an antiaromatic character, which destabilizes the coplanar conformation. A simple Hückel molecular orbital treatment³³ for the whole TTF molecule confirms that the neutral π -conjugated system is destabilized due to the electron occupation on an antibonding orbital. This is also reflected in the C=C bond lengths (1.35 Å), which are much closer to the C=C bond length in ethylene (1.33 Å) than in benzene (1.40 Å).

Adsorption of a Single TTF Molecule on Cu(100). Among the possible adsorption positions, we will only discuss the most stable ones. Thus, two different configurations describing adsorption of a TTF molecule on Cu(100) have been considered. In the first configuration, hereafter called the “lying-down” configuration, the molecular “plane” lies more or less parallel to the surface plane, as shown in Figure 5a. In the second configuration, hereafter called the “standing-up” configuration, the molecular plane is nearly perpendicular to the surface plane, as illustrated in Figure 5b. For the “lying-down” adsorption, the sulfur atoms are on top of the copper atoms, while for the “standing-up” adsorption, each sulfur atom is bound to two copper atoms. In the “lying-down” configuration, there are two kinds of molecule-metal bonding interactions: S—Cu and C—Cu bonds, as shown in Figure 5a. Bader’s topological analysis of the electron density further confirms the existence of C—Cu and S—Cu bonding interactions by the presence

of bond critical points (BCPs). Similar C—Cu bond formation has also been observed for other molecules adsorbed on Cu(110) surfaces.^{34,35}

Comparison of the reported geometries of Figure 5 with calculations using the same methods, but not including the vdW correction, shows that the inclusion of vdW correction significantly modifies the equilibrium geometry. In particular, the molecule stays much closer to the substrate after including vdW interactions. For instance, the S—Cu distance is shortened from 2.39 Å to 2.32 Å in the case of the “standing-up” configuration (see Table 1).

At the same time, the vdW correction leads to important changes in the adsorption energies. From Table 1, we can see that, for the “lying-down” configuration, the vdW contribution is 45.3 kcal/mol, thus leading to an increase of the adsorption energy by approximately a factor of 4. A similar increase is obtained when one uses the converged DFT geometries to evaluate the DFT adsorption energy (from 15.3 to 59.7 kcal/mol). For the “standing-up” configuration, the conclusion is the same. In this case, the vdW contribution is smaller: 27.0 kcal/mol. The fact that

vdW effects are much more important in the “lying-down” structure than in the “standing-up” one is due to the fact that, in the former, the molecule is closer to the substrate. Therefore, it can be concluded that the long-range dispersion correction to the total energy is crucial to obtain correct total and relative adsorption energies.

In the “standing-up” configuration, the most favorable adsorption site for sulfur is the bridge site, and the adsorbed molecule takes a nearly planar instead of a boat-like conformation. The different preference of adsorption site between the “lying-down” and the “standing-up” configurations is due to different bonding situations for sulfur atoms. Each sulfur atom utilizes four sp^3 -hybridized orbitals to form covalent bonds and/or to accommodate its lone pairs. These four sp^3 orbitals are oriented in space as a tetrahedral arrangement. In the “lying-down” configuration, the lone pairs of sulfur are directed either to the surface or the vacuum, therefore forming only one covalent bond. In the “standing-up” configuration, each sulfur atom stays at the bridge site of the surface and forms two S—Cu bonds. Similar differences in the site preference have also been observed for TTF adsorbed on the Au(111) surface.³⁶

Nevertheless, as we will see in the next section, the “standing-up” configuration becomes the most stable one when the self-assembly is considered. It is evident from Figure 5 that both the internal bonds in TTF and the interaction with the surface are very different in the “standing-up” and the “lying-down” configurations. As the aim of this paper is to analyze the self-assembly observed in the experiments, a more detailed analysis of single-molecule adsorption characteristics will be presented elsewhere.

Adsorption of Self-Assembled TTF on Cu(100). Let us discuss now the adsorption of self-assembled TTF on Cu(100) surface. As in the case of single-molecule adsorption, both “lying-down” and “standing-up” configurations are considered in the self-assembled model as starting points of the optimizations. As mentioned above, in this model, a 2×5 unit cell compatible with the experimental observations is used. It turns out that, when one starts with the “lying-down” adsorption mode, the molecule

Table 1. Calculated Adsorption Energies E_{ads} (in kcal/mol per molecule) and S—Cu Distances $d_{\text{S—Cu}}$ (in Å) for TTF Adsorbed at the Cu(100) Surface

system	$E_{\text{ads}}^{\text{DFT}^e}$	$E_{\text{ads}}^{\text{vdW}^e}$	$E_{\text{ads}}^{\text{DFT+vdW}^e}$	$E_{\text{ads}}^{\text{DFT-opt}^f}$	$d_{\text{S—Cu}}^{\text{DFT+vdW}^e}$	$d_{\text{S—Cu}}^{\text{DFT-opt}^f}$
sing-L ^a	14.4	45.3	59.7	15.3	2.30	2.32
sing-S ^b	11.1	27.0	38.2	10.7	2.32	2.39
assem-P ^c	9.0	28.8	37.8	9.2 ^g	2.32	2.42 ^g
assem-T ^d	10.3	29.3	39.6	11.5 ^g	2.30	2.36 ^g

^a Single TTF adsorbed at Cu(100) with the “lying-down” configuration.

^b Single TTF adsorbed at Cu(100) with the “standing-up” configuration.

^c Self-assembled TTF adsorbed at Cu(100) with the perpendicular configuration.

^d Self-assembled TTF adsorbed at Cu(100) with the tilted configuration.

^e At the DFT-D optimized geometry.

^f At the DFT optimized geometry.

^g Using a $4 \times 2 \times 1$ k-point mesh.

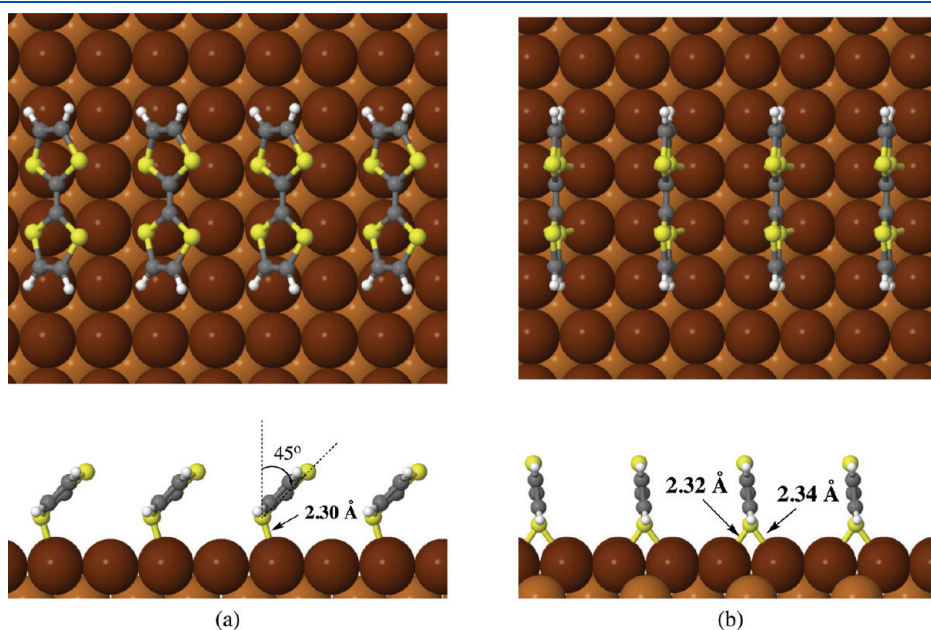


Figure 6. DFT-D optimized geometry of a self-assembled chain of TTF on Cu(100) surface. (a) Tilted configuration “assem-T”. (b) Perpendicular configuration “assem-P”. The upper and lower panels show a top and a side view, respectively. The optimized bond length and tilt angle in the equilibrium geometry are also shown.

evolves toward a “standing up” configuration during the structure relaxation, but this evolution eventually stops leading to a tilted equilibrium geometry (denoted as “assem-T” hereafter) as illustrated in Figure 6a. The tilt angle is approximately 45° with respect to the surface normal. In contrast, when one starts from the “standing-up” configuration, the molecule remains perpendicular to the substrate after geometry optimization. This structure is referred to as the “assem-P” configuration hereafter. In both cases, the molecule remains neutral (Bader’s analyses show a charge transfer of about $0.01 e^-$). Therefore, charge repulsion between neighboring molecules cannot be invoked to explain why the observed chains are short.

The “assem-T” configuration is energetically more stable than the “assem-P” configuration. This is the consequence of two effects. The first effect is the stronger vdW interaction between tilted neighboring molecules than between vertical neighboring molecules.

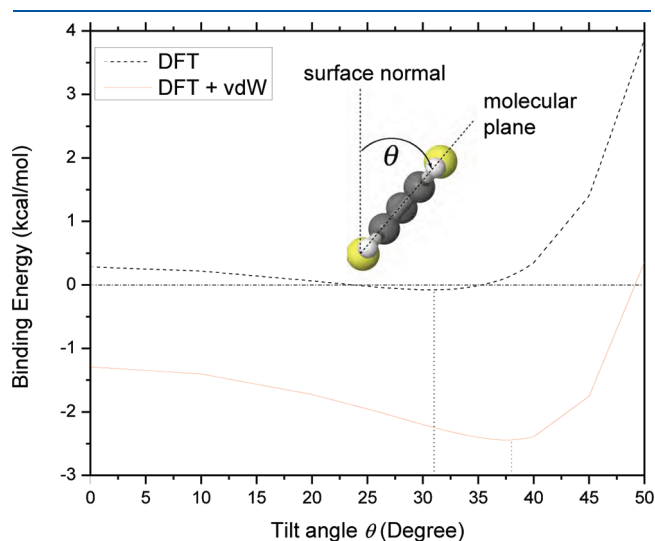


Figure 7. Binding energy per molecule as a function of tilt angle θ . The binding energy is calculated for a periodic chain of planar TTF molecules spaced by 5.1 Å in gas phase. Solid and dashed lines indicate the results with and without vdW correction, respectively.

To understand this point, we have modeled a periodic molecular chain of TTF in gas phase. In this model, we have considered that molecules are neutral and planar, since the molecules carry almost zero charge and are nearly planar in both the “assem-T” and “assem-P” configurations. They are aligned in vacuum, with a spacing between consecutive neighbors of about 5.1 Å, the same distance as in our calculations for self-assembled TTF on Cu(100). Then we have evaluated the binding energy per molecule as a function of tilt angle, defined as the angle between the molecule’s plane and the surface normal (see the inset in Figure 7). The results are shown in Figure 7. As can be seen, the binding energy per molecule has a minimum at around 38° , in reasonable agreement with the value of the tilt angle (45°) for TTF self-assembled on Cu(100). The stabilization energy per molecule due to the molecular tilting is about 1.2 kcal/mol. This value is reasonable since the difference in the total vdW contribution between the “assem-T” and the “assem-P” arrangements is 0.5 kcal/mol (see Table 1). A similar phenomenon has also been observed in self-assembled monolayers of alkanethiolates.^{23,37} Figure 7 also demonstrates that the standard DFT method without vdW correction gives almost zero interaction for tilt angles ranging from zero to the optimal value. This result shows that the binding between neighboring TTF molecules in the chain mainly comes from vdW interactions. This is confirmed by the fact that the binding energy (2.4 kcal/mol) of “assem-T” in gas phase is similar to the difference (2.3 kcal/mol) of the adsorption energies from vdW contribution between “assem-T” and “sing-S” (see Table 1).

The second effect is surface reconstruction, which is less important in “assem-T” than in “assem-P”. As shown in Figure 8a, in the relaxed topmost layer of the clean Cu(100) surface, the distance between nearest-neighbor copper atoms is 2.57 Å. However, in the “assem-P” adsorption model, the distances between neighboring copper atoms are alternatively elongated and shortened to 2.65 and 2.50 Å, respectively (see Figure 8c). Rearrangement of surface atoms is less important in the “assem-T” adsorption model, since the corresponding distances are 2.62 and 2.54 Å, respectively (see Figure 8d). Therefore, “assem-P” is more destabilized than “assem-T”. Table 1 shows that the DFT contribution to the adsorption energy per atom for “assem-T” is 1.3 kcal/mol larger than that for “assem-P”.

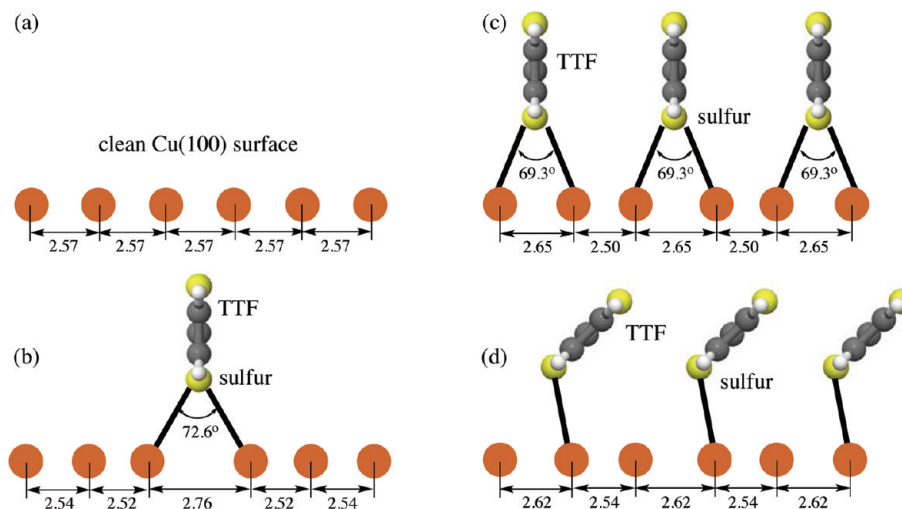


Figure 8. Variation of lattice distances (in Å) of the topmost layer of Cu(100) surface. (a) Clean surface. (b) Adsorption of a single molecule with the “standing-up” configuration. (c) Adsorption of self-assembled molecules with perpendicular configuration “assem-P”. (d) Adsorption of self-assembled molecules with tilted configuration “assem-T”.

The formation energy of the periodic molecular chain on the surface can be defined as the difference of adsorption energies between “assem-T” and “sing-S”. As can be seen in Table 1, the chain formation energy is estimated to be about 1.4 kcal/mol per molecule. This value is much smaller than the formation energy (2.4 kcal/mol per molecule) of the corresponding periodic chain in gas phase as shown in Figure 7. This is due to the energy cost to produce the surface reconstruction, but also to the strain of the sulfur–metal bonds. Indeed, as illustrated in Figure 8, for an isolated TTF molecule adsorbed at the bridge site of the surface, the distance between the two neighboring copper atoms bonded to sulfur is 2.74 Å, a value significantly larger than that of the lattice constant of the clean surface (2.57 Å). Although this stress is alleviated to some extent by rearrangement of the surrounding surface atoms, in the case of a periodic chain bonded to the surface, the surface atoms are rearranged collectively (see Figure 8c and d), and consequently the stress cannot be released all along the chain direction. In the case of “assem-P”, the distance between the two copper atoms bridged by sulfur cannot be as large as in the isolated TTF at surface. In this case, as shown in Figure 8b and c, the Cu–S–Cu bond angle is reduced from 72.6° to 69.3°. Therefore, both the stress of the surface and the less favorable molecule–substrate interactions lead to chain formation energies smaller at the surface than in the gas phase. As the total surface stress will be smaller for short than for long self-assembled chains, one can reasonably expect that chain formation will be more exothermic for short chains. This might explain why only short chains are observed in the experiments.

CONCLUSIONS

We have investigated adsorption and self-assembly of TTF molecules on Cu(100) surfaces, by using STM and performing DFT calculations that include vdW corrections following Grimme's DFT-D scheme. The experiments show the formation of short chains of self-assembled TTF molecules that disappear after annealing at high temperature.

The calculations show that isolated TTF molecules chemisorb on Cu(100), with an adsorption energy of about 59.7 kcal/mol, lying down on the surface with four sulfur atoms and four carbon atoms bonded to copper. The vdW interaction between the adsorbate and the substrate is responsible for most of the total adsorption energy. Another possible but energetically less favorable adsorption mode for isolated molecules corresponds to molecules lying perpendicular to the substrate with two sulfur atoms on the same side bonded at bridge sites of the surface.

The calculations also show that perpendicularly adsorbed TTF molecules can be further stabilized by forming 1D chains. This self-assembly pattern is mainly explained by the vdW interaction between molecules that are tilted away from the surface normal by about 45°. For this tilt angle, the intermolecular interaction is maximum. The formation energy of an infinite TTF chain on Cu(100) is about 1.4 kcal/mol per molecule. This value is expected to be larger for short chains where the surface atoms are less stressed upon adsorption of TTF. This could explain why only short chains are observed in the experiments. The total adsorption energy of the infinite TTF chain on Cu(100) is 39.6 kcal/mol per molecule, much smaller than that for single-molecule adsorption. Hence, TTF chains lying on the substrate are metastable, which explains why the chains disappear after annealing at higher temperatures.

In summary, the formation of short TTF chains on Cu(100) surface results from the interplay between molecule–molecule and molecule–substrate interactions. The formation of the chains is mainly due to intermolecular vdW interactions. The size of the chains is restricted, which might be due to the surface stress induced by the molecule–metal interactions.

AUTHOR INFORMATION

Corresponding Author

*E-mail: yang.wang@uam.es. Phone: +34 914978471. Fax: +34 914975238.

ACKNOWLEDGMENT

We thank Mare Nostrum BSC and CCC-UAM for computer time. Work supported by the MICINN projects FIS2010-15127, FIS2010-18847, ACI2008-0777, CTQ2010-17006, CT2008-00795, Consolider-Ingenio CSD2007-00010, and the CAM program NANOBIOIMAGNET S2009/MAT1726.

REFERENCES

- (1) Yu, G.; Gao, J.; Hummelen, J. C.; Wudl, F.; Heeger, A. J. *Science* **1995**, 270, 1789.
- (2) Halls, J. J. M.; A. Walsh, C.; Greenham, N. C.; Marseglia, E. A.; Friend, R. H.; Morati, S. C.; Holmes, A. B. *Nature* **1995**, 376, 498.
- (3) Günes, S.; Neugebauer, H.; Sariciftci, N. S. *Chem. Rev.* **2007**, 107, 1324.
- (4) Delgado, J. L.; Bouit, P.-A.; Filippone, S.; Herranz, M. A.; Martín, N. *Chem. Commun.* **2010**, 46, 4853.
- (5) Feyter, S. D.; Schryver, F. C. D. *Chem. Soc. Rev.* **2003**, 32, 139.
- (6) Barth, J. V.; Costantini, G.; Kern, K. *Nature* **2005**, 437.
- (7) Otero, R.; Rosei, F.; Besenbacher, F. *Annu. Rev. Phys. Chem.* **2006**, 57, 497.
- (8) Coleman, L. B. *Solid State Commun.* **1973**, 12, 1125.
- (9) Fernandez-Torrente, I.; Monturet, S.; Franke, K. J.; Fraxedas, J.; Lorente, N.; Pascual, J. I. *Phys. Rev. Lett.* **2007**, 99, 176103.
- (10) Hofmann, O. T.; Rangger, G. M.; Zojer, E. *J. Phys. Chem. C* **2008**, 112, 20357.
- (11) Martorell, B.; Clotet, A.; Fraxedas, J. *J. Comput. Chem.* **2010**, 15, 1842.
- (12) Martorell, B.; Fraxedas, J.; Clotet, A. *Surf. Sci.* **2011**, 605, 187.
- (13) Urban, C.; Écija, D.; Wang, Y.; Trelka, M.; Preda, I.; Vollmer, A.; Lorente, N.; Arnau, A.; Alcam, M.; Soriano, L.; Martn, N.; Martín, F.; Otero, R.; Gallego, J. M.; Miranda, R. *J. Phys. Chem. C* **2010**, 114, 6503.
- (14) Mercurio, G.; McNellis, E. R.; Martin; Hagen, S.; Leyssner, F.; Soubatch, S.; Meyer, J.; Wolf, M.; Tegeder, P.; Tautz, F. S.; Reuter, K. *Phys. Rev. Lett.* **2010**, 104, 036102.
- (15) Kresse, G.; Hafner, J. *Phys. Rev. B* **1994**, 49, 14251.
- (16) Kresse, G.; Furthmüller, J. *Phys. Rev. B* **1996**, 54, 11169.
- (17) Kresse, G.; Furthmüller, J. *Comput. Mater. Sci.* **1996**, 6, 15.
- (18) Kresse, G.; Joubert, D. *Phys. Rev. B* **1999**, 59, 1758.
- (19) Blöchl, P. E. *Phys. Rev. B* **1994**, 50, 17953.
- (20) Perdew, J. P.; Burke, W.; Ernzerhof, M. *Phys. Rev. Lett.* **1996**, 77, 3965.
- (21) Methfessel, M.; Paxton, A. *Phys. Rev. B* **1989**, 40, 3616.
- (22) Monkhorst, H. J.; Pack, J. D. *Phys. Rev. B* **1976**, 13, 5188.
- (23) Canchaya, J. G. S.; Wang, Y.; Busnengo, H.; Alcam, M.; Martn, F. *Phys. Chem. Chem. Phys.* **2010**, 12, 7555.
- (24) Grimme, S. *J. Comput. Chem.* **2006**, 27, 1787.
- (25) Straumanis, M. E.; Yu, L. S. *Acta Crystallogr., Sect. A* **1969**, 25, 676.
- (26) Bader, R. F. W. *Acc. Chem. Res.* **1985**, 18, 9.
- (27) Bader, R. F. W. *Atoms in Molecules—A Quantum Theory*; Oxford: London, 1990.
- (28) Bader, R. F. W. *Chem. Rev.* **1991**, 91, 893.

- (29) Arnaldsson, A.; Tang, W.; Henkelman, G. Bader analysis program. <http://theory.cm.utexas.edu/vtsttools/bader/>
- (30) Pou-Amérgo, R.; Viruela, P. M.; Viruela, R.; Rubio, M.; Ortí, E. *Chem. Phys. Lett.* **2002**, 352, 491.
- (31) Pou-Amérgo, R.; Ortí, E.; Merchán, M.; Rubio, M.; Viruela, P. M. *J. Phys. Chem. A* **2002**, 106, 631.
- (32) Hargittai, I.; Brunvoll, J.; Kolonits, M.; Khodorkovsky, V. J. *Mol. Struct.* **1994**, 317, 273.
- (33) Coulson, C. A.; O'Leary, B.; Mallion, R. B. *Hückel Theory for Organic Chemists*; Oxford, Academic Press: London, 1978.
- (34) Atodiresei, N.; Caciuc, V.; Lazić, P.; Blüge, S. *Phys. Rev. Lett.* **2009**, 102, 136809.
- (35) Ji, W.; Zotti, L. A.; Gao, H.-J.; Hofer, W. A. *Phys. Rev. Lett.* **2010**, 104, 099703.
- (36) Fueno, H.; Hayashi, M.; Nin, K.; Kubo, A.; Misaki, Y.; Tanaka, K. *Curr. Appl. Phys.* **2006**, 6, 939.
- (37) Abufager, P. N.; Canchaya, J. G. S.; Wang, Y.; Alcamí, M.; Martín, F.; Soria, L. A.; Martiarena, M. L.; Reuter, K.; Busnengo, H. *Phys. Chem. Chem. Phys.* **2011**, 13, 9353.